

**Stochastic Analysis of Two-Phase Flow
in Heterogeneous Media
by Combining Karhunen-Loeve Expansion and
Perturbation Method**

Mingjie Chen^{1,2}, Dongxiao Zhang², Arturo A. Keller¹, and Zhiming Lu²

1. Bren School of Environmental Sciences and Management, University of California, Santa Barbara, CA
2. Hydrology, Geochemistry, and Geology Group (EES-6), Los Alamos National Laboratory, NM

For submission to *Water Resources Research*
June 01, 2004

Abstract

We present a novel approach to modeling stochastic multiphase flow problems, for example NAPL flow, in a heterogeneous subsurface medium with random soil properties, in particular, with randomly heterogeneous intrinsic permeability and soil grain size. A stochastic model for steady state water-oil flow in two-dimensional random field is developed using the Karhunen-Loeve Moment Equation (KLME) approach and is numerically implemented. An exponential model is adopted to define the constitutive relationship between phase relative permeability and capillary pressure. The log-transformed intrinsic permeability $Y(\mathbf{x})$ and soil pore size distribution $\beta(\mathbf{x})$ are assumed to be Gaussian random functions with a separable exponential covariance function. The perturbation part of these two log-transformed soil properties is then decomposed into an infinite series based on a set of orthogonal normal random variables $\{\xi_n\}$. The phase pressure, capillary pressure and phase mobility are decomposed by polynomial expansions and perturbation method. Combining these expansions of $Y(\mathbf{x})$, $\beta(\mathbf{x})$ and dependent pressures, the steady state water-oil flow equations and corresponding boundary conditions are reformulated as a series of differential equations up to 2nd order. These differential equations are solved numerically and the solutions are directly used to construct moments of phase pressure and capillary pressure. We demonstrate the validity of the proposed KLME model by favorably comparing 1st and 2nd order approximations to Monte Carlo simulations. The significant computational efficiency of the KLME approach over Monte Carlo simulation is also illustrated.

1. Introduction

Non-Aqueous Phase Liquids (NAPLs), such as chlorinated solvents, hydrocarbon fuels, and polychlorinated biphenyls, have been used extensively in private industry, military installations and Department of Energy (DOE) facilities. NAPLs may be leaking from a damaged or decaying storage vessel (e.g. in a gasoline station, refinery, dry-cleaning operation), improperly constructed storage and distribution systems, a waste disposal lagoon, or may be spilt during transport and use in a manufacturing process (e.g. during degreasing of metal parts, in the electronics industry to clean semiconductors, or in an airfield for cleaning jet engines). NAPL spills during transport and leaks from underground storage tanks have inevitably occurred and represent a major risk to water supply, since even a small amount of NAPLs can contaminate large volumes of groundwater. NAPL ganglia (blobs) trapped in the porous soil or rock matrix at residual saturation are a continuous source of contamination to the aquifer or the soil vapor, through dissolution or vaporization (Garg *et al.*, 1999).

To design a remediation scheme, it is important to understand at a basic level the physicochemical processes that control the movement and mass transfer of NAPLs in the subsurface, both in the unsaturated and the water-saturated regions. The conceptual models of a typical contaminant spill into porous and fractured media have been put forward by several researchers (Abriola, 1989; Mercer *et al.*, 1990; Keller *et al.*, 2000). In some cases, the contaminant is dissolved in water and thus travels through the aquifer as a solute. More typically a contaminant enters the subsurface as a liquid phase separated from the gaseous or aqueous phases present. NAPLs travel first through the unsaturated

zone, under three-phase (water, air, oil) flow conditions, displacing air and water. The variations in matrix permeability and capillarity, due to the heterogeneity of the porous medium, result in additional deviations from vertical flow. Under some situation, less permeable layers (e.g. silt or clay lenses, or even tightly packed sand), or materials with smaller pores will make NAPL flow mostly in horizontal direction, until it encounters a path of less resistance. Microfractures in the soil matrix are also important in allowing the NAPL to flow through low-permeability lenses (Keller *et al.*, 2000). NAPLs are trapped within the porous medium when the capillary forces are sufficiently strong to overcome the viscous and gravitational forces acting on the NAPLs.

From this simplified description of the processes occurring as a NAPL moves through the subsurface, it is clear that soil heterogeneity plays a major role in the distribution of the spill, as well as in the transfer of NAPL mass to the surrounding phases (e.g. Keller and Chen, 2002). It is critical to understand how these processes are enhanced or limited by large variations in soil properties, including absolute permeability, porosity, fraction of organic content, capillary pressure-saturation and relative permeability-saturation relationships, soil density, etc. These properties may be treated as random space functions and the equations governing multiphase flow in these formations become stochastic. Solving the stochastic multiphase flow equations is a challenging task.

In the last two decades, stochastic approaches to flow and transport in heterogeneous porous media have been extensively studied and developed, which are summarized by Dagan (1989), Gelhar (1993) and Zhang (2002). The most common approach is to solve such stochastic flow equations numerically by Monte Carlo simulation. Using this technique, a large number of equally probable random realizations of the soil properties

are generated using geostatistical techniques such as Gaussian sequential simulation. The flow equations can be solved numerically by a conventional deterministic numerical flow simulator for each realization, and the moments of the flow system output can be obtained by averaging the results from all realizations. This approach is conceptually straightforward, but it requires intensive computational effort since the number of realizations needed to adequately describe the flow system is relatively high. Moreover, the computational effort for each realization is large in order to solve high space-time fluctuations in random parameters with fine numerical space-time grids. Therefore, Monte Carlo simulations are primarily used as a comparative reference for direct methods of solution of stochastic flow equations, which allow one to compute statistical moments of hydrogeologic variables, such as fluid pressure and velocity, without the need for generating a large number of realizations of these variables.

One direct approach is to formulate integro-differential moment equations with the aid of Green's function, make some approximations and then solve the equations numerically. The idea is to apply the perturbation scheme first, and then write moment equations based on a Green's function. This approach has been used extensively in the literature of flow in porous media (Dagan, 1989; Rubin and Dagan, 1988, 1989; Cheng and Lefe, 1991). Recently, exact integro-differential moment equations have been developed for steady state and transient flows in saturated porous media by Neuman and coworkers (Neuman and Orr, 1993; Tartakovsky and Neuman 1998; Guadagnini and Neuman, 1999). However, these equations cannot be solved without Monte Carlo simulations or closure approximations.

Another direct approach is to derive a system of partial differential moment equations governing the statistical moments of flow quantities in a straightforward manner and then solve them analytically or numerically. The moment equations are formulated based on perturbation expansion approaches (Bakr *et al.*, 1978; Gutjahr *et al.*, 1981). Analytical solutions to the differential moment equations of flow are available only for some special cases such as uniform mean flow in unbounded media (Dagan, 1989; Gelhar, 1993) and uniform mean flow in rectangular domains of stationary media (Osnes, 1995). For real-world applications with complex flow configurations, and boundary conditions, numerical methods have to be employed to solve the differential moment equations (Zhang, 1998).

Compared to Monte Carlo simulation, direct approaches provide a more comprehensive and efficient method for analyzing flow system in heterogeneous media by representing the entire flow system by several stochastic parameters. Most of the previous and current stochastic modeling via direct methods have focused on steady or transient saturated flow, and single phase unsaturated flow. Little work has been done on stochastic modeling of these properties under the condition of multiphase flow, both due to the nonlinear character of the governing equations and their interdependence, as well as due to lack of extensive field data of properties representing spatial variability. Data limitations are being addressed by new advances in soil characterization technologies, for example using multiprobe cone penetrometers, geophysical methods, and inter-phase partitioning tracers (e.g. Kram *et al.*, 2000). Several researchers have recently proposed a few stochastic analyses of multiphase flow. Chang *et al.* (1995) and Abdin *et al.* (1997a, 1997b) presented a spectral/perturbation approach to analyze two- and three-phase flow

stochastically. Ghanem *et al.* (1998) applied Karhunen-Loeve decomposition technology and polynomial chaos expansion to stochastic variables of two-phase flow and solved the corresponding moments numerically.

Zhang and coworkers (Zhang, 1998, 1999; Zhang and Sun, 2000; Zhang and Lu, 2002) proposed the moment equation method based on a perturbation analysis by translating stochastic partial differential equations to partial differential moment equations, and solving them numerically. Recently, Zhang and Lu (2004) combined Karhunen-Loeve decomposition with Moment Equation methods, i.e., KLME, to obtain higher-order (>1) approximations of the hydraulic head and flux for saturated flow in randomly heterogeneous porous media, and solved the resulting equations numerically. Yang, *et al.* (2004) then applied KLME to saturated-unsaturated one-phase flow. In contrast with the polynomial chaos method (Ghanmen, 1998) and the conventional moment equation method (Zhang, 1998), the KLME method solves the deterministic coefficients of the dependent variable expansion series in different orders, and then constructs moments of the variables in different orders instead of solving the covariance equations. The KLME method has proven to be more efficient computationally than Monte Carlo and CME approach for saturated water flow and unsaturated water flow (Lu and Zhang, 2004; Yang *et al.*, 2004).

In this paper, we implement KLME for a two-phase (water-oil) steady-state flow system. Both the intrinsic permeability and pore size distribution are considered stochastic soil properties. Thus, we address the challenging issue of stochastic permeability and capillary pressures. First, we derive the differential equations using the KLME approach, and then we discretize and code them in a numerical solver called

STO-2PHASE. We then obtain higher orders of the moments of stochastic output variables. Finally, we conduct two cases studies and perform a comparable Monte Carlo simulation in order to evaluate the limitations and validity of the KLME method applied in this study.

2. Mechanics of two-phase flow in porous media

We consider a steady water-oil flow in unsaturated porous media. The porous medium and fluids are considered incompressible and under isothermal conditions. The conservation equations and Darcy's relationship can be written as (Bear, 1972):

$$\begin{aligned}\nabla \cdot \mathbf{q}_w(\mathbf{x}) &= 0, \\ \nabla \cdot \mathbf{q}_o(\mathbf{x}) &= 0,\end{aligned}\tag{1}$$

$$\begin{aligned}\mathbf{q}_w(\mathbf{x}) &= -\lambda_w [\nabla \cdot P_w(\mathbf{x}) + \rho_w \mathbf{g}], \\ \mathbf{q}_o(\mathbf{x}) &= -\lambda_o [\nabla \cdot P_o(\mathbf{x}) + \rho_o \mathbf{g}],\end{aligned}\tag{2}$$

subject to boundary conditions

$$P_w(\mathbf{x}) = P_{w0}(\mathbf{x}), \quad P_o(\mathbf{x}) = P_{o0}(\mathbf{x}), \quad \mathbf{x} \in \Gamma_D, \tag{3}$$

$$\mathbf{q}_w(\mathbf{x}) \cdot \mathbf{n}(\mathbf{x}) = Q_w(\mathbf{x}), \quad \mathbf{q}_o(\mathbf{x}) \cdot \mathbf{n}(\mathbf{x}) = Q_o(\mathbf{x}), \quad \mathbf{x} \in \Gamma_N, \tag{4}$$

where $\lambda_w = k(\mathbf{x})k_{rw}(S_w)/\mu_w$ and $\lambda_o = k(\mathbf{x})k_{ro}(S_o)/\mu_o$ are water and oil phase mobility; \mathbf{q}_i is the water ($i = w$) and oil ($i = o$) flux; \mathbf{x} is the position vector in 2- or 3-D; P_i is the i phase pressure; ρ_i is the i phase density; k_{ri} is the i phase relative permeability; μ_i is the i phase dynamic viscosity; P_{i0} is the constant i phase pressure on the Dirichlet boundary segment Γ_D ; Q_i is the constant i phase flux across Neuman boundary segments Γ_N ; S_i is the i phase saturation; \mathbf{g} is the gravity vector; k is the intrinsic permeability of porous media; \mathbf{n} is the outward unit vector normal to the boundary Γ_N .

Letting $Z_w(\mathbf{x}) = \ln \lambda_w(\mathbf{x})$, $Z_o(\mathbf{x}) = \ln \lambda_o(\mathbf{x})$, and combining (1) and (2) gives the governing flow equations as:

$$\frac{\partial^2 P_w(\mathbf{x})}{\partial x_i^2} + \frac{\partial Z_w(\mathbf{x})}{\partial x_i} \left[\frac{\partial P_w(\mathbf{x})}{\partial x_i} + \rho_w g \delta_{i1} \right] = 0, \quad (5)$$

$$\frac{\partial^2 P_o(\mathbf{x})}{\partial x_i^2} + \frac{\partial Z_o(\mathbf{x})}{\partial x_i} \left[\frac{\partial P_o(\mathbf{x})}{\partial x_i} + \rho_o g \delta_{i1} \right] = 0, \quad (6)$$

subject to boundary conditions

$$P_w(\mathbf{x}) = P_{w0}(\mathbf{x}), \quad P_o(\mathbf{x}) = P_{o0}(\mathbf{x}), \quad \mathbf{x} \in \Gamma_D, \quad (7)$$

$$\begin{aligned} n_i(\mathbf{x}) \exp[Z_w(\mathbf{x})] \left[\frac{\partial P_w(\mathbf{x})}{\partial x_i} + \rho_w g \delta_{i1} \right] &= -Q_w(\mathbf{x}), \\ n_i(\mathbf{x}) \exp[Z_o(\mathbf{x})] \left[\frac{\partial P_o(\mathbf{x})}{\partial x_i} + \rho_o g \delta_{i1} \right] &= -Q_o(\mathbf{x}), \end{aligned} \quad \mathbf{x} \in \Gamma_N, \quad (8)$$

where δ_{i1} is the Kröneckner delta function, which equals 1 when i is 1 (upward direction) or 0 otherwise.

The constitutive relationships of relative permeability k_{rw} , k_{ro} versus saturation S or capillary pressure P_c have to be specified. Empirical instead of theoretical relationships are commonly used. There are several postulated models, for example those based on van Genuchten's relationships (1980). Here we adopt exponential-type constitutive relationships similar to those used by Chang *et al.* (1995):

$$k_{rw} = \exp[-\alpha_c \beta_c P_c], \quad k_{ro} = 1 - \exp[-\alpha_c \beta_c P_c], \quad (9)$$

where α_c is the soil grain size distribution index; β_c is the ratio of water surface tension to oil-water interfacial tension, and is considered as a deterministic constant, depending only on fluid properties. Typically the assumption is made that soil properties (k , α_c) are

homogenous in the domain, which might seriously under- or over-predict the movement of NAPLs, and thus provides an inaccurate understanding of the extent of contamination.

In this study, we treat k and α_c as random fields subject to log normal distribution. For mathematical simplicity, let $\alpha = \alpha_c \beta_c$ and $\ln \alpha = \beta$, then the relative permeabilities can be expressed as

$$k_{rw} = \exp[-\alpha P_c] = \exp[-\exp(\beta) P_c], \quad (10)$$

$$k_{ro} = 1 - \exp[-\alpha P_c] = 1 - \exp[-\exp(\beta) P_c]. \quad (11)$$

The exponential functional relationship is used given that it allows a tractable solution to the flow equations. Abidin *et al.* (1997b) verified the applicability of these constitutive relationships in a series of comparisons with the widely used van Genuchten model (van Genuchten, 1980) using real soil properties. Their results indicate a reasonable agreement between these two models.

The difficulty in solving these stochastic equations (5) and (6) by Monte Carlo approach is the intensive computational effort since these are typically very large (many grid blocks are required for an accurate solution) matrix systems of highly nonlinear, discrete equations and large number of realizations required in MC. For this reason, we would like to resort to direct stochastic approaches instead of Monte Carlo methods to solve the stochastic multiphase flow system.

3. Karhunen-Loeve expansion of intrinsic permeability

It has been known for a long time that there is a close connection between stochastic processes and orthogonal polynomials (Wiener, 1930). The approximate solution techniques based on classical orthogonal polynomials are generally known as spectral

methods. Karhunen-Loeve (KL) expansion of a stochastic process $\alpha(\mathbf{x}, \theta)$, which was derived by several investigators independently (Karhunen, 1947; Loeve, 1948), is based on the spectral decomposition of the covariance function of α , $C_{\alpha\alpha}(\mathbf{x}, \mathbf{y})$, with a set of orthogonal polynomials (Courant and Hilbert, 1953). Here, \mathbf{x} and \mathbf{y} indicate spatial locations, while the argument θ denotes the random nature of the corresponding quantity. Ghanem and Dham (1998) applied the KL expansion to decompose the log-transformed intrinsic permeability of the medium assuming normal distribution: $Y(\mathbf{x}, \theta) = \ln[k(\mathbf{x}, \theta)]$, where k is the intrinsic permeability, \mathbf{x} is the position in spatial domain \mathbf{D} , and θ belongs to the probability space Ω . The log-transformed permeability can be written as: $Y(\mathbf{x}, \theta) = \langle Y(\mathbf{x}, \theta) \rangle + Y'(\mathbf{x}, \theta)$, where, $\langle \cdot \rangle$ denotes the expected mean operator, and $Y'(\mathbf{x}, \theta)$ represents the fluctuations around the mean. Then, the covariance of log intrinsic permeability can be expressed as $C_Y(\mathbf{x}, \mathbf{y}) = \langle Y'(\mathbf{x}, \theta) Y'(\mathbf{y}, \theta) \rangle$. $C_Y(\mathbf{x}, \mathbf{y})$ is bounded, symmetrical and positive definite, and hence can be decomposed as

$$C_Y(\mathbf{x}, \mathbf{y}) = \sum_{n=1}^{\infty} \lambda_n f_n(\mathbf{x}) f_n(\mathbf{y}), \quad (12)$$

where λ_n and $f_n(\mathbf{x})$ are the eigenvalues and eigenvectors of the covariance kernel, respectively. Eigenvalues and eigenvectors can be solved from the integral equation

$$\int_D C_Y(\mathbf{x}, \mathbf{y}) f(\mathbf{x}) d\mathbf{x} = \lambda f(\mathbf{y}). \quad (13)$$

Owing to the symmetry and positive definiteness of the covariance function (Loeve, 1977), the eigenvectors are orthogonal and form a complete set:

$$\int_D f_n(\mathbf{x}) f_m(\mathbf{x}) d\mathbf{x} = \delta_{nm}, \quad (14)$$

where δ_{nm} is the Krönecker delta function.

The perturbation part of log intrinsic permeability can be expanded in terms of eigenfunctions as:

$$Y'(\mathbf{x}, \theta) = \sum_{n=1}^{\infty} \xi_n(\theta) \sqrt{\lambda_n} f_n(\mathbf{x}) \quad , \quad (15)$$

where $\{\xi_n(\theta)\}$ forms a set of orthogonal random variables, and has properties of $\langle \xi_n(\theta) \rangle = 0$, and $\langle \xi_n(\theta) \xi_m(\theta) \rangle = \delta_{nm}$. Because $Y(\mathbf{x}, \theta)$ is assumed Gaussian distributed, $\xi_i(\theta)$ forms a Gaussian vector, and any subset of $\xi_i(\theta)$ is jointly Gaussian.

$$\langle \xi_1(\theta) \cdots \xi_{2n+1}(\theta) \rangle = 0, \quad (16)$$

$$\langle \xi_1(\theta) \cdots \xi_{2n}(\theta) \rangle = \sum_{i,j=1}^{2n} \prod \langle \xi_i(\theta) \xi_j(\theta) \rangle. \quad (17)$$

For some special types of covariance functions, analytical solution of eigenvalues and eigenfunctions can be found from (13). In general cases, they have to be solved numerically via iterative methods or a Galerkin-type method (Ghanem and Spanos, 1991).

The eigenvalues decrease monotonically, guaranteed by the symmetry of the covariance function (Ghanem and Dham, 1998). The rate of decay is subject to the correlation length of the intrinsic permeability field, i.e. the shorter the correlation length; the more terms are required in the expansions. Zhang and Lu (2004) discussed this issue in detail in their application of KLME to saturated flow.

4. Two-phase flow KL-based moment equations (KLME)

Zhang and Lu (2004) pioneered the combination of the KL method with high-order perturbation methods to set up KL-based Moment Equations (KLME) for saturated flow. In this section, we apply the KLME approach to steady-state two-phase (water-oil) flow, to derive higher-order approximations for the mean and variance of phase pressures.

The log-transformed phase mobility, $Z_w(\mathbf{x}) = \ln \lambda_w(\mathbf{x})$, and $Z_o(\mathbf{x}) = \ln \lambda_o(\mathbf{x})$ can be written as:

$$Z_w(\mathbf{x}) = \ln \lambda_w(\mathbf{x}) = Y(\mathbf{x}) - \ln \mu_w - \exp[\beta(\mathbf{x})] P_c(\mathbf{x}), \quad (18)$$

$$Z_o(\mathbf{x}) = \ln \lambda_o(\mathbf{x}) = Y(\mathbf{x}) - \ln \mu_o + \ln \left\{ 1 - \exp[-\exp[\beta(\mathbf{x})] P_c(\mathbf{x})] \right\}. \quad (19)$$

The phase pressures, capillary pressure and phase mobility can be expressed as infinite series:

$$\begin{aligned} P_w(\mathbf{x}) &= P_w^{(0)}(\mathbf{x}) + P_w^{(1)}(\mathbf{x}) + P_w^{(2)}(\mathbf{x}) + \dots, \\ P_o(\mathbf{x}) &= P_o^{(0)}(\mathbf{x}) + P_o^{(1)}(\mathbf{x}) + P_o^{(2)}(\mathbf{x}) + \dots, \\ P_c(\mathbf{x}) &= P_c^{(0)}(\mathbf{x}) + P_c^{(1)}(\mathbf{x}) + P_c^{(2)}(\mathbf{x}) + \dots, \end{aligned} \quad (20)$$

$$\begin{aligned} Z_w(\mathbf{x}) &= Z_w^{(0)}(\mathbf{x}) + Z_w^{(1)}(\mathbf{x}) + Z_w^{(2)}(\mathbf{x}) + \dots, \\ Z_o(\mathbf{x}) &= Z_o^{(0)}(\mathbf{x}) + Z_o^{(1)}(\mathbf{x}) + Z_o^{(2)}(\mathbf{x}) + \dots, \end{aligned} \quad (21)$$

where $P_w^{(n)}$, $P_o^{(n)}$, $P_c^{(n)}$ are terms of order σ_s^n in a statistically sense. σ_s is the standard deviation of $s = k, \beta$. $Z_w^{(n)}$ and $Z_o^{(n)}$ ($n = 0, 1, 2$) are presented in Appendix A.

Substituting (20) and (21) into (5) and (6), and collecting terms at the same order generates the differential equations for each order:

Zeroth-order differential equations:

$$\begin{aligned} \frac{\partial^2 P_w^{(0)}(\mathbf{x})}{\partial x_i^2} + \frac{\partial Z_w^{(0)}(\mathbf{x})}{\partial x_i} \left[\frac{\partial P_w^{(0)}(\mathbf{x})}{\partial x_i} + \rho_w g \delta_{il} \right] &= 0, \\ \frac{\partial^2 P_o^{(0)}(\mathbf{x})}{\partial x_i^2} + \frac{\partial Z_o^{(0)}(\mathbf{x})}{\partial x_i} \left[\frac{\partial P_o^{(0)}(\mathbf{x})}{\partial x_i} + \rho_o g \delta_{il} \right] &= 0, \end{aligned} \quad (22)$$

with boundaries

$$P_w^{(0)}(\mathbf{x}) = P_{w0}(\mathbf{x}), \quad P_o^{(0)}(\mathbf{x}) = P_{o0}(\mathbf{x}), \quad \mathbf{x} \in \Gamma_D, \quad (23)$$

$$\begin{aligned}
n_i(\mathbf{x}) \left[\frac{\partial P_w^{(0)}(\mathbf{x})}{\partial x_i} + \rho_w g \delta_{il} \right] &= \frac{-Q_w(\mathbf{x})}{\exp[Z_w^{(0)}(\mathbf{x})]}, \\
n_i(\mathbf{x}) \left[\frac{\partial P_o^{(0)}(\mathbf{x})}{\partial x_i} + \rho_o g \delta_{il} \right] &= \frac{-Q_o(\mathbf{x})}{\exp[Z_o^{(0)}(\mathbf{x})]},
\end{aligned}
\quad \mathbf{x} \in \Gamma_N. \quad (24)$$

First-order differential equations:

$$\begin{aligned}
\frac{\partial^2 P_w^{(1)}(\mathbf{x})}{\partial x_i^2} + \frac{\partial Z_w^{(1)}(\mathbf{x})}{\partial x_i} \left[\frac{\partial P_w^{(0)}(\mathbf{x})}{\partial x_i} + \rho_w g \delta_{il} \right] + \frac{\partial Z_w^{(0)}(\mathbf{x})}{\partial x_i} \frac{\partial P_w^{(1)}(\mathbf{x})}{\partial x_i} &= 0, \\
\frac{\partial^2 P_o^{(1)}(\mathbf{x})}{\partial x_i^2} + \frac{\partial Z_o^{(1)}(\mathbf{x})}{\partial x_i} \left[\frac{\partial P_o^{(0)}(\mathbf{x})}{\partial x_i} + \rho_o g \delta_{il} \right] + \frac{\partial Z_o^{(0)}(\mathbf{x})}{\partial x_i} \frac{\partial P_o^{(1)}(\mathbf{x})}{\partial x_i} &= 0,
\end{aligned}
\quad (25)$$

with boundaries

$$P_w^{(1)}(\mathbf{x}) = 0, \quad P_o^{(1)}(\mathbf{x}) = 0, \quad \mathbf{x} \in \Gamma_D, \quad (26)$$

$$\begin{aligned}
n_i(\mathbf{x}) \left[\frac{\partial P_w^{(1)}(\mathbf{x})}{\partial x_i} + J_{wi}(\mathbf{x}) Z_w^{(1)}(\mathbf{x}) \right] &= 0, \\
n_i(\mathbf{x}) \left[\frac{\partial P_o^{(1)}(\mathbf{x})}{\partial x_i} + J_{oi}(\mathbf{x}) Z_o^{(1)}(\mathbf{x}) \right] &= 0,
\end{aligned}
\quad \mathbf{x} \in \Gamma_N, \quad (27)$$

where $J_{wi}(\mathbf{x}) = \partial P_w^{(0)}(\mathbf{x}) / \partial x_i + \rho_w g \delta_{il}$ and $J_{oi}(\mathbf{x}) = \partial P_o^{(0)}(\mathbf{x}) / \partial x_i + \rho_o g \delta_{il}$.

Second-order differential equations:

$$\begin{aligned}
\frac{\partial^2 P_w^{(2)}(\mathbf{x})}{\partial x_i^2} + \frac{\partial Z_w^{(2)}(\mathbf{x})}{\partial x_i} \left[\frac{\partial P_w^{(0)}(\mathbf{x})}{\partial x_i} + \rho_w g \delta_{il} \right] + \frac{\partial Z_w^{(1)}(\mathbf{x})}{\partial x_i} \frac{\partial P_w^{(1)}(\mathbf{x})}{\partial x_i} + \frac{\partial Z_w^{(0)}(\mathbf{x})}{\partial x_i} \frac{\partial P_w^{(2)}(\mathbf{x})}{\partial x_i} &= 0, \\
\frac{\partial^2 P_o^{(2)}(\mathbf{x})}{\partial x_i^2} + \frac{\partial Z_o^{(2)}(\mathbf{x})}{\partial x_i} \left[\frac{\partial P_o^{(0)}(\mathbf{x})}{\partial x_i} + \rho_o g \delta_{il} \right] + \frac{\partial Z_o^{(1)}(\mathbf{x})}{\partial x_i} \frac{\partial P_o^{(1)}(\mathbf{x})}{\partial x_i} + \frac{\partial Z_o^{(0)}(\mathbf{x})}{\partial x_i} \frac{\partial P_o^{(2)}(\mathbf{x})}{\partial x_i} &= 0,
\end{aligned}
\quad (28)$$

with boundaries

$$P_w^{(2)}(\mathbf{x}) = 0, \quad P_o^{(2)}(\mathbf{x}) = 0, \quad \mathbf{x} \in \Gamma_D, \quad (29)$$

$$\begin{aligned}
n_i(\mathbf{x}) \left[\frac{\partial P_w^{(2)}(\mathbf{x})}{\partial x_i} + Z_w^{(1)}(\mathbf{x}) \frac{\partial P_w^{(1)}(\mathbf{x})}{\partial x_i} + J_{wi}(\mathbf{x}) Z_w^{(2)}(\mathbf{x}) \right] &= 0, \\
n_i(\mathbf{x}) \left[\frac{\partial P_o^{(2)}(\mathbf{x})}{\partial x_i} + Z_o^{(1)}(\mathbf{x}) \frac{\partial P_o^{(1)}(\mathbf{x})}{\partial x_i} + J_{oi}(\mathbf{x}) Z_o^{(2)}(\mathbf{x}) \right] &= 0,
\end{aligned}
\quad \mathbf{x} \in \Gamma_N. \quad (30)$$

We assume that $P_w^{(1)}(\mathbf{x})$, $P_o^{(1)}(\mathbf{x})$ can be expanded in terms of a set of orthogonal Gaussian random variables ξ_n , $n = 1, 2, \dots$, as defined in the Karhunen-Loeve decomposition:

$$P_w^{(1)}(\mathbf{x}) = \sum_{n=1}^{\infty} \xi_n P_{w,n}^{(1)}(\mathbf{x}), \quad P_o^{(1)}(\mathbf{x}) = \sum_{n=1}^{\infty} \xi_n P_{o,n}^{(1)}(\mathbf{x}), \quad (31)$$

where $P_{w,n}^{(1)}(\mathbf{x})$ and $P_{o,n}^{(1)}(\mathbf{x})$ are deterministic functions to be determined.

To simplify the mathematical representation using KLME, we rewrite (15) as:

$$Y'(\mathbf{x}, \theta) = \sum_{n=1}^{\infty} \xi_n(\theta) \sqrt{\lambda_n} f_n(\mathbf{x}) = \sum_{n=1}^{\infty} \xi_n(\theta) \overline{f_n}(\mathbf{x}), \quad (32)$$

where $\sqrt{\lambda_n}$ is included in $\overline{f_n}(\mathbf{x})$, since eigenvalues and eigenfunctions are always coupled. To simplify mathematical expression, we will write $\overline{f_n}(\mathbf{x})$ as $f_n(\mathbf{x})$ in the following formulation. Likewise, the KL expansion of $\beta'(\mathbf{x})$ is:

$$\beta'(\mathbf{x}, \theta) = \sum_{n=1}^{\infty} \xi_n(\theta) \phi_n(\mathbf{x}), \quad (33)$$

where $\phi_n(\mathbf{x})$, like $f_n(\mathbf{x})$, is the set of eigenfunctions of the covariance matrix of $\beta(\mathbf{x})$.

Substituting (31), (32), (33) and $Z_w^{(1)}(\mathbf{x})$, $Z_o^{(1)}(\mathbf{x})$ (Appendix A) and their spatial derivatives into (25) yields the infinite series in terms of ξ_n , whose summation equals zero. For example, the water phase equation in (25) becomes:

$$\sum_{n=1}^{\infty} \xi_n \left\{ \frac{\partial^2 P_{w,n}^{(1)}}{\partial x_i^2} + \left(\frac{\partial \langle Y \rangle}{\partial x_i} - \alpha_G \frac{\partial P_c^{(0)}}{\partial x_i} - P_c^{(0)} \frac{\partial \alpha_G}{\partial x_i} \right) \frac{\partial P_{w,n}^{(1)}}{\partial x_i} \right. \\ \left. - J_{wi} \left(\alpha_G \frac{\partial P_{c,n}^{(1)}}{\partial x_i} - P_{c,n}^{(1)} \frac{\partial \alpha_G}{\partial x_i} \right) + J_{wi} \left[\frac{\partial f_n}{\partial x_i} - P_c^{(0)} \phi_n \frac{\partial \alpha_G}{\partial x_i} - P_c^{(0)} \alpha_G \frac{\partial \phi_n}{\partial x_i} - \alpha_G \phi_n \frac{\partial P_c^{(0)}}{\partial x_i} \right] \right\} = 0. \quad (34)$$

Owing to the orthogonality and independence of the set ξ_n , $n = 1, 2, \dots$, all coefficients of this infinite series have to be zero, which results in:

$$\frac{\partial^2 P_{w,n}^{(1)}}{\partial x_i^2} + \left[\frac{\partial \langle Y \rangle}{\partial x_i} - \alpha_G \frac{\partial P_c^{(0)}}{\partial x_i} - P_c^{(0)} \frac{\partial \alpha_G}{\partial x_i} \right] \frac{\partial P_{w,n}^{(1)}}{\partial x_i} \\ = J_{wi} \left(\alpha_G \frac{\partial P_{c,n}^{(1)}}{\partial x_i} - P_{c,n}^{(1)} \frac{\partial \alpha_G}{\partial x_i} \right) - J_{wi} \left(\frac{\partial f_n}{\partial x_i} - P_c^{(0)} \phi_n \frac{\partial \alpha_G}{\partial x_i} - P_c^{(0)} \alpha_G \frac{\partial \phi_n}{\partial x_i} - \alpha_G \phi_n \frac{\partial P_c^{(0)}}{\partial x_i} \right), \quad (35)$$

with boundaries

$$P_{w,n}^{(1)}(\mathbf{x}) = 0, \quad \mathbf{x} \in \Gamma_D, \quad (36)$$

$$n_i(\mathbf{x}) \left[\frac{\partial P_{w,n}^{(1)}(\mathbf{x})}{\partial x_i} + J_{wi}(\mathbf{x}) Z_{w,n}^{(1)}(\mathbf{x}) \right] = 0, \quad \mathbf{x} \in \Gamma_N. \quad (37)$$

Similarly, we can obtain the KLME for the oil pressure.

$$\frac{\partial^2 P_{o,n}^{(1)}}{\partial x_i^2} + \left[\frac{\partial \langle Y \rangle}{\partial x_i} + a \alpha_G \frac{\partial P_c^{(0)}}{\partial x_i} + a P_c^{(0)} \frac{\partial \alpha_G}{\partial x_i} \right] \frac{\partial P_{o,n}^{(1)}}{\partial x_i} \\ = -J_{oi} \left(a P_{c,n}^{(1)} \frac{\partial \alpha_G}{\partial x_i} + a \alpha_G \frac{\partial P_{c,n}^{(1)}}{\partial x_i} + \alpha_G P_{c,n}^{(1)} \frac{\partial a}{\partial x_i} \right) \\ - J_{oi} \left(\frac{\partial f_n}{\partial x_i} + a \alpha_G \phi_n \frac{\partial P_c^{(0)}}{\partial x_i} + a \alpha_G P_c^{(0)} \frac{\partial \phi_n}{\partial x_i} + a \phi_n P_c^{(0)} \frac{\partial \alpha_G}{\partial x_i} + \alpha_G \phi_n P_c^{(0)} \frac{\partial a}{\partial x_i} \right), \quad (38)$$

with boundaries

$$P_{o,n}^{(1)}(\mathbf{x}) = 0, \quad \mathbf{x} \in \Gamma_D, \quad (39)$$

$$n_i(\mathbf{x}) \left[\frac{\partial P_{o,n}^{(1)}(\mathbf{x})}{\partial x_i} + J_{oi}(\mathbf{x}) Z_{o,n}^{(1)}(\mathbf{x}) \right] = 0, \quad \mathbf{x} \in \Gamma_N, \quad (40)$$

where the decomposed first order phase mobilities are given from (A-7):

$$\begin{aligned} Z_{w,n}^{(1)}(\mathbf{x}) &= f_n - \alpha_G (P_{c,n}^{(1)} + \phi_n P_c^{(0)}), \\ Z_{o,n}^{(1)}(\mathbf{x}) &= f_n + a\alpha_G (P_{c,n}^{(1)} + \phi_n P_c^{(0)}). \end{aligned} \quad (41)$$

According to the definitions of $f_n(\mathbf{x})$ and $\phi_n(\mathbf{x})$, all the driving terms in (35), (38) are proportional to eigenvalues of covariance functions of intrinsic permeability and pore size distribution, which decrease monotonically as n increases. This guarantees that the contributions of $P_{w,n}^{(1)}$ to $P_w^{(1)}$, and $P_{o,n}^{(1)}$ to $P_o^{(1)}$ decrease with n . The KLME derivation of the second order pressures, $P_w^{(2)}$, and $P_o^{(2)}$, is presented in the Appendix B.

Up to second-order in σ_s , fluid pressure is approximated by

$$P_w(\mathbf{x}) \approx \sum_{i=0}^2 P_w^{(i)}(\mathbf{x}), \quad P_o(\mathbf{x}) \approx \sum_{i=0}^2 P_o^{(i)}(\mathbf{x}). \quad (42)$$

For the water pressure, the mean is approximated by

$$\langle P_w(\mathbf{x}) \rangle \approx \langle P_w^{(0)}(\mathbf{x}) \rangle + \langle P_w^{(1)}(\mathbf{x}) \rangle + \langle P_w^{(2)}(\mathbf{x}) \rangle = P_w^{(0)}(\mathbf{x}) + \sum_{j=1}^{\infty} P_{w,jj}^{(2)}(\mathbf{x}) \quad (43)$$

From (42) and (43), the second order perturbation terms can be written as

$$P'_w(\mathbf{x}) = P_w(\mathbf{x}) - \langle P_w(\mathbf{x}) \rangle \approx P_w^{(1)}(\mathbf{x}) + P_w^{(2)}(\mathbf{x}) - \langle P_w^{(2)}(\mathbf{x}) \rangle \quad (44)$$

The covariance of $P_w(\mathbf{x}), P_w(\mathbf{y})$ can be derived as

$$C_{P_w}(\mathbf{x}, \mathbf{y}) = \sum_{n=1}^{\infty} P_{w,n}^{(1)}(\mathbf{x}) P_{w,n}^{(1)}(\mathbf{y}) + 2 \sum_{j,k=1}^{\infty} P_{w,jk}^{(2)}(\mathbf{x}) P_{w,jk}^{(2)}(\mathbf{y}) \quad (45)$$

The covariance between Y, β and P_w or P_o , cross-covariance between P_w and P_o can be constructed in a similar manner.

One of the superiorities of the KLME approach relative to other stochastic methods is that, once we obtain $P_{w,i_1,i_2,\dots,i_l}^{(l)}(\mathbf{x})$, $P_{o,i_1,i_2,\dots,i_l}^{(l)}(\mathbf{x})$, $l = 0, 1, 2, \dots$, we can directly compute

the high-order mean and covariance of each phase pressure without solving equations for covariance and cross-covariance of phase pressure, log relative permeability required in the CME methods, hence it is more efficient computationally.

5. Numerical Implementation

The zeroth-order equations (22) are nonlinear and the first, second-order KLME (35, 38, B-2, B-3) equations are coupled, and cannot be solved analytically. We use a finite difference scheme to solve them numerically.

The final discretized equations can be expressed as

$$\mathbf{A}\mathbf{P} = \mathbf{R} \quad (46)$$

where \mathbf{A} is the coefficient matrix, \mathbf{P} is the solution vector for $P_w^{(0)}, P_{w,n}^{(1)}, P_{w,jk}^{(2)}$ and $P_o^{(0)}, P_{o,n}^{(1)}, P_{o,jk}^{(2)}$, and \mathbf{R} is a vector containing information about the RHS (right hand side) of each equation and the boundary conditions. The matrix \mathbf{A} is the same for problem sets in different orders and only needs to be decomposed once. The driving force \mathbf{R} has to be substituted as many times as the number of different RHS vectors. The zeroth-order flow equations are nonlinear and coupled, and need to be solved in an iterative manner. The first- and second-order equations are linear but coupled, and also need necessary iterations to converge. The zeroth-order solution needs more iteration than the first- and second-order solutions to converge, because the zeroth-order equations are nonlinear while the higher-order equations are linear. Solving the higher-order equations requires all the lower-order solutions. This two-dimensional finite difference scheme for stochastic two-phase flow has been implemented into a computer Fortran code called “STO-2PHASE”. Currently, this code is capable of handling steady-state two-phase flow, with regular non-uniform grids features.

6. Illustrative Examples

Two examples are used to illustrate the validity of this approach for stochastic water-oil flow in heterogeneous soil. In both cases the log-transformed intrinsic permeability Y and pore size distribution parameter β are assumed to be second-order stationary with a separable exponential covariance function:

$$C_{\omega}(\mathbf{x}, \mathbf{y}) = \sigma_{\omega}^2 \exp\left(-\frac{|x_1 - y_1|}{\eta_{\omega 1}} - \frac{|x_2 - y_2|}{\eta_{\omega 2}}\right) \quad (47)$$

where $\omega = Y$ or β , σ_{ω}^2 is the variance of ω , and $\eta_{\omega i}$ is the correlation length of ω in the i th direction.

6.1 Baseline case

In this first case, we start by determining how many first-order and second-order terms are sufficient to capture the uncertainty of the soil properties, and then show the validity of the proposed stochastic KLME model by comparing the KLME results to the Monte-Carlo simulation. We consider a rectangular grid of 16×50 square elements in a vertical cross section (Fig. 1) having a height of 3.0 m and a width of 0.96 m. The size of elements is 0.06 m \times 0.06 m. The boundary condition are specified as follows: (1) no flow at left and right sides ($x_2 = 0$, $x_2 = 0.96$ m); (2) constant deterministic water and oil infiltration rates Q_w , Q_o at the top ($x_1 = 3.0$ m); and (3) water and oil phase pressure P_w , P_o specified at the bottom of the domain. The input parameters are given in Table 1.

To investigate the number of terms that are sufficient to capture the uncertainty of the random field, and yet as few as possible to reduce the computational effort, we designed a series of numerical simulations with different number of the first-order terms (term1) and second-order terms (term2). Because capillary pressure is the coupled element between water phase and oil phase flow equations, as well as the key parameter in phase relative permeability model, the validity of capillary pressure solution can demonstrate sufficiently the validity of the output of the whole flow system. Fig. 2 (a) shows a series of variance of capillary pressure along the central vertical line with term1 = 100, 150, 200, 300, and 500 while fixing the number of the second-order terms to 60. There is little difference between the results from term1 = 300 and term1 = 500, compared with the differences among term1 = 100, 150, 200 and 300. It is apparent that increasing term1 beyond 300 contributes little to explaining capillary pressure variance. Fixing term1 = 300, we ran a series of simulations with term2 = 60, 70, 80, 90, 100, and 120. Fig. 2 (b) presents the results. Beyond term2 = 100, the variance of capillary pressure increases only slightly. Thus, the combination of term1 = 300 and term2 = 100 was chosen for KLME method for the comparison against Monte Carlo simulation.

To test the validity of the KLME approach and the numerical implementation, we conducted 2000 Monte Carlo simulations. 2,000 2-D random soil properties fields were generated with the separable covariance function (47) using the Gaussian Sequential Simulation approach available in GSLIB (Deutsch and Journel, 1998). The deterministic solver solved the 2,000 water, oil pressure and capillary pressure fields, and statistical moments were calculated based on these fields. These statistics are considered true solutions that are used as a reference to compare our KLME approach at various orders.

As shown in Figure 3, the second-order KLME results match the MC simulation very well and improve on the lower-order solutions.

Fig. 4 presents contour maps of water, oil and capillary pressure means. The means of water and oil pressure are specified at the lower boundary, and increase upward along the vertical direction approximately linearly. The capillary pressure decreases with elevation, and remains almost constant in the area near the upper boundary, which is similar to gravity dominated flow (water) in unsaturated flow system. The central vertical section of the capillary pressure in Fig. 3 clearly indicates this kind of trend.

Fig. 5 presents contour maps of water, oil and capillary pressure variances. The variances are zero at the bottom boundary of constant pressure and increase in the vertical direction upward. In the horizontal direction, the pressure variances are largest at the two lateral boundaries and decrease toward the center of the domain, especially for capillary pressure. The behavior of capillary pressure variances in this case (water-oil) is similar to the head variance under steady state unsaturated flow (Zhang and Winter, 1998).

The number of terms required to approximate $P_{w,n}^{(1)}, P_{w,jk}^{(2)}$ and $P_{o,n}^{(1)}, P_{o,jk}^{(2)}$ determine the computational effort of the KLME approach. As discussed above, we took 300 and 100 terms for the first and second order, respectively. To obtain $P_{w,i_1,i_2,\dots,i_m}^{(m)}$, where $i_j = \overline{1,n}$, the number of times required to solve an equation is $S_m = n(n+1)\cdots(n+m-1)/m!$. In our case, when $m = 1$, $n = 300$, so we need to solve the first-order equations for $S_1 = 300$ times, while $S_2 = 100*(100+1)/2 = 5050$ times for $m=2$. Unlike saturated and unsaturated one phase flow, this two-phase flow is a coupled system, so that solving the linear discretized first- and second-order equations also requires a number of iterations. With the particular solver that we used, solving for the zeroth-order solution needs about 50

iterations, whereas the first- and second-order solutions usually converge after 5 iterations each, so the total number of runs for KLME is about $50+5*(300+5050) = 26,800$. With a similar solver, each realization of the Monte Carlo (MC) simulation converges after about 100 iterations, since the parameter fields are not so smooth as in the KLME approach. Thus, 200,000 iterations are required for 2,000 MC simulations, which is nearly 8 times of the effort in the KLME approach. The actual run time for KLME is 1-2 hours, while MC simulation requires 1-2 days in the same computer. For a larger domain, the increased simulation time might be quite significant.

6.2 Case2: Larger σ_Y^2

In this second case, we increase the variance of the log-transformed intrinsic permeability, σ_Y^2 , from 0.25 (intrinsic permeability Coefficient of Variation, CV = 53%) to 0.81 (CV = 112%). The large infiltration along with high permeability variance may cause divergence problem in the Monte Carlo simulations, so we decrease both water and oil infiltration to 1.0×10^{-10} m/s. Fig. 6 presents the comparison of mean and variance of capillary pressure between up to second-order KLME simulations and 4,000 Monte Carlo simulations along the central vertical section. Under this larger σ_Y^2 , more Monte Carlo realizations (4,000) are required for the statistical moments to converge, while only more 100 terms of the first-order (term1) are required for the KLME approach, hence the computing efficiency of the KLME approach over Monte Carlo approach is more apparent. As expected, the higher the order (0th, 1st or 2nd) of the KLME, the better the approximation to the Monte Carlo statistics. However, with the increase in σ_Y^2 , the differences among the Monte Carlo simulation, the first- and second-order KLME are

greater than those in smaller σ_Y^2 . The behavior of capillary pressure doesn't appear to have a gravity-dominated flow regime as in Case 1, due to the smaller fluid infiltrations. However, the vertical spatial gradient of capillary pressure decreases significantly with elevation.

Fig.7 and Fig. 8 present the contour map of means and variances of fluid pressures and capillary pressure using the KLME approach. Owing to the smaller infiltration rate at the top boundary, the mean water, oil pressures decrease upward vertically, instead of increasing as in Case 1. However, with gravitational force, the flow is still downward for water and oil. Capillary pressure decreases as in Case 1. Generally, large fluxes or large variances of soil random variables will lead to large pressure head variances. The variance of oil pressure shown in Fig. 8 is about 4 orders of magnitude smaller than that in Case 1, because the oil infiltration rate is 1/240 of Case 1 (1.0×10^{-10} m/s versus 2.4×10^{-8} m/s), while σ_Y^2 increase only by a factor of 3. The water pressure and capillary pressure variances change little from Case 1, because the water infiltration rate is similar to the first example (1.0×10^{-10} m/s vs. 6.8×10^{-9} m/s) and the effect of σ_Y^2 increase on water pressure variance can overcome the effect of water infiltration decrease.

7. Summary and Conclusions

A stochastic two-phase flow model was developed based on Karhunen-Loeve and polynomial expansions to evaluate higher-order moments for two-phase flow in randomly heterogeneous subsurface zone. The log-transformed intrinsic permeability $Y(\mathbf{x})$ and the soil pore size distribution parameter $\beta(\mathbf{x})$ were assumed to be Gaussian random functions with the separable exponential covariance functions. $Y(\mathbf{x})$ and $\beta(\mathbf{x})$ were first decomposed

into the infinite series related to the eigenvalues and eigenfunctions of the covariance functions of $Y(\mathbf{x})$ and $\beta(\mathbf{x})$ as well as a set of standard Gaussian random variables $\{\xi_n\}$ by Karhunen-Loeve expansions. Then, the fluid pressure and capillary pressure were decomposed into the series whose terms $P_w^{(n)}, P_o^{(n)}, P_c^{(n)}$ are n^{th} order in terms of σ_Y or σ_β . We then further expanded $P_w^{(n)}, P_o^{(n)}, P_c^{(n)}$ into series in terms of the product of n Gaussian random variables used in Karhunen-Loeve expansion of $Y(\mathbf{x})$ and $\beta(\mathbf{x})$, which leads to sets of equations for calculating the deterministic coefficients in these expansions. We developed a numerical code for the stochastic model and solve these coefficients, which were used to compute moments of fluid pressure and capillary pressure directly. We demonstrated the KLME approach with two cases of steady-state water-oil flow in a two-dimensional rectangular domain and compared the results with those from Monte Carlo simulations. The main findings of this paper are summarized as follows:

1. The KLME method is applicable to stochastic analysis of multiphase flow and this makes it possible to evaluate higher-order flow moments with smaller computational effort.
2. The KLME for two-phase flow was numerically implemented into a Fortran code STO-2PHASE, which can be used as a stochastic analysis tool for steady state two-phase flow and offers a template for further expansion of features, such as transient flow, three-phase flow, and other multiphase flow applications.
3. The comparison of KLME results with Monte Carlo simulations indicates that this proposed stochastic approach and the executable model produce very similar results, and the KLME approach is much more efficient than MC simulations.

4. Unlike saturated or unsaturated flow, the water-oil two-phase flow is a coupled system, so all the zeroth-, first- and second-order equations need several iterations to converge on a solution. However, the first- and second-order discretized equations are linear and require less iteration than the zeroth-order equations, which are nonlinear. In addition, the left hand coefficient matrix is the same in zeroth-, first- and second-order perturbations equations. These features make the numerical modeling very efficient because it is not necessary to rebuild the coefficient matrix for different orders of the perturbation equations in every iteration calculation.

The KLME approach is likely to have a significant application in large and complex heterogeneous multiphase systems, where uncertainty analysis requires new approaches to understand the implications of these non-linear, coupled systems.

Appendix A

According to (18), (19),

$$\begin{aligned} Z_w(\mathbf{x}) &= \ln \lambda_w(\mathbf{x}) = Y(\mathbf{x}) - \ln \mu_w - \exp[\beta(\mathbf{x})] P_c(\mathbf{x}), \\ Z_o(\mathbf{x}) &= \ln \lambda_o(\mathbf{x}) = Y(\mathbf{x}) - \ln \mu_o + \ln \left\{ 1 - \exp \left[-\exp[\beta(\mathbf{x})] P_c(\mathbf{x}) \right] \right\}. \end{aligned} \quad (\text{A-1})$$

$Y(\mathbf{x})$ and $\beta(\mathbf{x})$ are the random inputs of the system and can be written as:

$$\begin{aligned} Y(\mathbf{x}) &= \langle Y(\mathbf{x}) \rangle + Y'(\mathbf{x}), \\ \beta(\mathbf{x}) &= \langle \beta(\mathbf{x}) \rangle + \beta'(\mathbf{x}), \end{aligned} \quad (\text{A-2})$$

where $\langle Y(\mathbf{x}) \rangle$ and $\langle \beta(\mathbf{x}) \rangle$ are the expected mean of $Y(\mathbf{x})$ and $\beta(\mathbf{x})$, and $Y'(\mathbf{x})$ and $\beta'(\mathbf{x})$ are the zero mean perturbation terms, which can be decomposed by the Karhunen-Loeve expansion presented in Section 3.

In (A-1),

$$\exp(\beta) = \exp(\langle \beta \rangle + \beta') = \exp(\langle \beta \rangle) \exp(\beta') = \alpha_G \left(1 + \beta' + \frac{\beta'^2}{2} \right), \quad (\text{A-3})$$

where $\alpha_G = \exp(\langle \beta \rangle)$, and $\exp(\beta')$ is approximated by Taylor expansion.

Substituting (A-2) and (A-3) into (A-1), one obtains a series of $Z(\mathbf{x})$ and their spatial derivative in different orders.

For the zero order,

$$\begin{aligned} Z_w^{(0)}(\mathbf{x}) &= \langle Y(\mathbf{x}) \rangle - \ln \mu_w - \alpha_G(\mathbf{x}) P_c^{(0)}(\mathbf{x}), \\ Z_o^{(0)}(\mathbf{x}) &= \langle Y(\mathbf{x}) \rangle - \ln \mu_o + \ln \left[1 - \exp \left(-\alpha_G(\mathbf{x}) P_c^{(0)}(\mathbf{x}) \right) \right], \end{aligned} \quad (\text{A-4})$$

and

$$\begin{aligned}\frac{\partial Z_w^{(0)}(\mathbf{x})}{\partial x_i} &= \frac{\partial \langle Y(\mathbf{x}) \rangle}{\partial x_i} - \alpha_G(\mathbf{x}) \frac{\partial P_c^{(0)}(\mathbf{x})}{\partial x_i} - P_c^{(0)}(\mathbf{x}) \frac{\partial \alpha_G(\mathbf{x})}{\partial x_i} \\ \frac{\partial Z_o^{(0)}(\mathbf{x})}{\partial x_i} &= \frac{\partial \langle Y(\mathbf{x}) \rangle}{\partial x_i} + a(\mathbf{x}) \left[\alpha_G(\mathbf{x}) \frac{\partial P_c^{(0)}(\mathbf{x})}{\partial x_i} + P_c^{(0)}(\mathbf{x}) \frac{\partial \alpha_G(\mathbf{x})}{\partial x_i} \right],\end{aligned}\quad (\text{A-5})$$

where

$$a(\mathbf{x}) = \frac{\exp[-\alpha_G(\mathbf{x})P_c^{(0)}(\mathbf{x})]}{1 - \exp[-\alpha_G(\mathbf{x})P_c^{(0)}(\mathbf{x})]}.\quad (\text{A-6})$$

To simplify the mathematical representation, we omit (\mathbf{x}) in the first- and second-order equations; however note that every term in these equations is a function of space node (\mathbf{x}) .

For the first order,

$$\begin{aligned}Z_w^{(1)}(\mathbf{x}) &= Y' - \alpha_G(P_c^{(1)} + \beta' P_c^{(0)}), \\ Z_o^{(1)}(\mathbf{x}) &= Y' + a\alpha_G(P_c^{(1)} + \beta' P_c^{(0)}),\end{aligned}\quad (\text{A-7})$$

and

$$\begin{aligned}\frac{\partial Z_w^{(1)}(\mathbf{x})}{\partial x_i} &= \frac{\partial Y'}{\partial x_i} - \alpha_G \left(\frac{P_c^{(1)}}{\partial x_i} + \beta' \frac{\partial P_c^{(0)}}{\partial x_i} + P_c^{(0)} \frac{\partial \beta'}{\partial x_i} \right) - \frac{\partial \alpha_G}{\partial x_i} (P_c^{(1)} + \beta' P_c^{(0)}) \\ \frac{\partial Z_o^{(1)}(\mathbf{x})}{\partial x_i} &= \frac{\partial Y'}{\partial x_i} + a\alpha_G \left(\frac{P_c^{(1)}}{\partial x_i} + \beta' \frac{\partial P_c^{(0)}}{\partial x_i} + P_c^{(0)} \frac{\partial \beta'}{\partial x_i} \right) + a \frac{\partial \alpha_G}{\partial x_i} (P_c^{(1)} + \beta' P_c^{(0)}) \\ &\quad + \frac{\partial a}{\partial x_i} \alpha_G [P_c^{(1)} + \beta' P_c^{(0)}].\end{aligned}\quad (\text{A-8})$$

For the second order,

$$\begin{aligned}Z_w^{(2)}(\mathbf{x}) &= -\alpha_G \left(P_c^{(2)} + \beta' P_c^{(1)} + \frac{\beta'^2}{2} P_c^{(0)} \right), \\ Z_o^{(2)}(\mathbf{x}) &= Z_{21} P_c^{(2)} + Z_{22} [P_c^{(1)}]^2 + Z_{23} \beta' P_c^{(1)} + Z_{24} [\beta']^2,\end{aligned}\quad (\text{A-9})$$

where

$$Z_{21}(\mathbf{x}) = a\alpha_G - a^2\alpha_G^2 P_c^{(0)},$$

$$Z_{22}(\mathbf{x}) = -\frac{1}{2}a\alpha_G^2 - \frac{1}{2}a^2\alpha_G^2,$$

$$Z_{23}(\mathbf{x}) = a\alpha_G - a\alpha_G^2 P_c^{(0)} - a^2\alpha_G^2 P_c^{(0)},$$

$$Z_{24}(\mathbf{x}) = \frac{1}{2}a\alpha_G P_c^{(0)} - \frac{1}{2}a\alpha_G^2 [P_c^{(0)}]^2 - \frac{1}{2}a^2\alpha_G^2 [P_c^{(0)}]^2,$$

and

$$\begin{aligned} \frac{\partial Z_w^{(2)}(\mathbf{x})}{\partial x_i} &= -\langle \alpha \rangle \frac{P_c^{(2)}}{\partial x_i} - P_c^{(2)} \frac{\partial \langle \alpha \rangle}{\partial x_i} - \alpha' \frac{P_c^{(1)}}{\partial x_i} - P_c^{(1)} \frac{\partial \alpha'}{\partial x_i} \\ \frac{\partial Z_o^{(2)}(\mathbf{x})}{\partial x_i} &= Z_{21} \frac{\partial P_c^{(2)}}{\partial x_i} + P_c^{(2)} dZ_{21} + 2Z_{22} P_c^{(1)} \frac{\partial P_c^{(1)}}{\partial x_i} + (P_c^{(1)})^2 dZ_{22} \\ &+ Z_{23} \left[\alpha' \frac{\partial P_c^{(1)}}{\partial x_i} + P_c^{(1)} \frac{\partial \alpha'}{\partial x_i} \right] + \alpha' P_c^{(1)} dZ_{23} + 2Z_{24} \alpha' \frac{\partial \alpha'}{\partial x_i} + (\alpha')^2 dZ_{24}, \end{aligned} \quad (\text{A-10})$$

where

$$\begin{aligned} dZ_{21} &= \frac{\partial Z_{21}}{\partial x_i} = \left(\alpha_G \frac{\partial a}{\partial x_i} + a \frac{\partial \alpha_G}{\partial x_i} \right) - \left(2\alpha_G^2 P_c^{(0)} a \frac{\partial a}{\partial x_i} + \alpha_G^2 a^2 \frac{\partial P_c^{(0)}}{\partial x_i} + 2\alpha_G a^2 P_c^{(0)} \frac{\partial \alpha_G}{\partial x_i} \right), \\ dZ_{22} &= \frac{\partial Z_{22}}{\partial x_i} = -\frac{1}{2} \left(\alpha_G^2 \frac{\partial a}{\partial x_i} + 2\alpha_G a \frac{\partial \alpha_G}{\partial x_i} \right) - \left(\alpha_G^2 a \frac{\partial a}{\partial x_i} + a^2 \alpha_G \frac{\partial \alpha_G}{\partial x_i} \right), \\ dZ_{23} &= \frac{\partial Z_{23}}{\partial x_i} = \left(\alpha_G \frac{\partial a}{\partial x_i} + a \frac{\partial \alpha_G}{\partial x_i} \right) - \left(\alpha_G^2 P_c^{(0)} \frac{\partial a}{\partial x_i} + a\alpha_G^2 \frac{\partial P_c^{(0)}}{\partial x_i} + 2a\alpha_G P_c^{(0)} \frac{\partial \alpha_G}{\partial x_i} \right) \\ &\quad - \left(2a\alpha_G^2 P_c^{(0)} \frac{\partial a}{\partial x_i} + \alpha_G^2 a^2 \frac{\partial P_c^{(0)}}{\partial x_i} + 2a^2 P_c^{(0)} \alpha_G \frac{\partial \alpha_G}{\partial x_i} \right), \\ dZ_{24} &= \frac{\partial Z_{24}}{\partial x_i} = \frac{1}{2} \left(a\alpha_G \frac{\partial P_c^{(0)}}{\partial x_i} + aP_c^{(0)} \frac{\partial \alpha_G}{\partial x_i} + \alpha_G P_c^{(0)} \frac{\partial a}{\partial x_i} \right) \\ &\quad - \left(2a\alpha_G^2 P_c^{(0)} \frac{\partial P_c^{(0)}}{\partial x_i} + 2a(P_c^{(0)})^2 \alpha_G \frac{\partial \alpha_G}{\partial x_i} + \alpha_G^2 (P_c^{(0)})^2 \frac{\partial a}{\partial x_i} \right) \\ &\quad - 2 \left(a^2 \alpha_G^2 P_c^{(0)} \frac{\partial P_c^{(0)}}{\partial x_i} + a^2 (P_c^{(0)})^2 \alpha_G \frac{\partial \alpha_G}{\partial x_i} + \alpha_G^2 (P_c^{(0)})^2 a \frac{\partial a}{\partial x_i} \right). \end{aligned}$$

APPENDIX B

Following the same steps as the derivation of the first order pressures, $P_w^{(1)}(\mathbf{x})$, $P_o^{(1)}(\mathbf{x})$,

we can expand $P_w^{(2)}, P_o^{(2)}$ in terms of $\xi_j \xi_k$ ($j \geq k \geq 1$).

$$P_w^{(2)}(\mathbf{x}) = \sum_{j,k=1}^{\infty} \xi_j \xi_k P_{w,jk}^{(2)}(\mathbf{x}), \quad P_o^{(2)}(\mathbf{x}) = \sum_{j,k=1}^{\infty} \xi_j \xi_k P_{o,jk}^{(2)}(\mathbf{x}). \quad (\text{B-1})$$

The 2nd order KLME equations can be derived from (28):

$$\begin{aligned} & \frac{\partial^2 P_{w,jk}^{(2)}}{\partial x_i^2} + \left[\frac{\partial \langle Y \rangle}{\partial x_i} - \alpha_G \frac{\partial P_c^{(0)}}{\partial x_i} - P_c^{(0)} \frac{\partial \alpha_G}{\partial x_i} \right] \frac{\partial P_{w,jk}^{(2)}}{\partial x_i} \\ &= J_{wi} \left(\alpha_G \frac{\partial P_{c,jk}^{(2)}}{\partial x_i} + P_{c,jk}^{(2)} \frac{\partial \alpha_G}{\partial x_i} \right) + \frac{1}{2} J_{wi} \left(\alpha_G \phi_j \frac{\partial P_{c,k}^{(1)}}{\partial x_i} + \alpha_G \phi_k \frac{\partial P_{c,j}^{(1)}}{\partial x_i} \right. \\ & \quad + \alpha_G P_{c,j}^{(1)} \frac{\partial \phi_k}{\partial x_i} + \alpha_G P_{c,k}^{(1)} \frac{\partial \phi_j}{\partial x_i} + \alpha_G \phi_j \phi_k \frac{\partial P_c^{(0)}}{\partial x_i} + \alpha_G \phi_j P_c^{(0)} \frac{\partial \phi_k}{\partial x_i} \\ & \quad \left. + \alpha_G \phi_k P_c^{(0)} \frac{\partial \phi_j}{\partial x_i} + \phi_j P_{c,k}^{(1)} \frac{\partial \alpha_G}{\partial x_i} + \phi_k P_{c,j}^{(1)} \frac{\partial \alpha_G}{\partial x_i} + \phi_j \phi_k P_c^{(0)} \frac{\partial \alpha_G}{\partial x_i} \right) \\ & \quad - \frac{1}{2} \frac{\partial P_{w,j}^{(1)}}{\partial x_i} \left(\frac{\partial f_k}{\partial x_i} - \frac{\partial \alpha_G}{\partial x_i} (P_{c,k}^{(1)} + \phi_k P_c^{(0)}) - \alpha_G \left(\frac{\partial P_{c,k}^{(1)}}{\partial x_i} + \phi_k \frac{\partial P_c^{(0)}}{\partial x_i} + P_c^{(0)} \frac{\partial \phi_k}{\partial x_i} \right) \right) \\ & \quad - \frac{1}{2} \frac{\partial P_{w,k}^{(1)}}{\partial x_i} \left(\frac{\partial f_j}{\partial x_i} - \frac{\partial \alpha_G}{\partial x_i} (P_{c,j}^{(1)} + \phi_j P_c^{(0)}) - \alpha_G \left(\frac{\partial P_{c,j}^{(1)}}{\partial x_i} + \phi_j \frac{\partial P_c^{(0)}}{\partial x_i} + P_c^{(0)} \frac{\partial \phi_j}{\partial x_i} \right) \right), \end{aligned} \quad (\text{B-2})$$

with boundaries

$$\begin{aligned} & P_{w,jk}^{(2)}(\mathbf{x}) = 0, \quad \mathbf{x} \in \Gamma_D, \\ & n_i(\mathbf{x}) \left[\frac{\partial P_{w,jk}^{(2)}(\mathbf{x})}{\partial x_i} + \frac{1}{2} \left(Z_{w,j}^{(1)}(\mathbf{x}) \frac{\partial P_{w,k}^{(1)}(\mathbf{x})}{\partial x_i} + Z_{w,k}^{(1)}(\mathbf{x}) \frac{\partial P_{w,j}^{(1)}(\mathbf{x})}{\partial x_i} \right) \right. \\ & \quad \left. + J_{wi}(\mathbf{x}) \left(Z_{w,jk}^{(2)}(\mathbf{x}) + \frac{1}{2} Z_{w,j}^{(1)}(\mathbf{x}) Z_{w,k}^{(1)}(\mathbf{x}) \right) \right] = 0, \quad \mathbf{x} \in \Gamma_N, \end{aligned}$$

$$\begin{aligned}
& \frac{\partial^2 P_{o,jk}^{(2)}}{\partial x_i^2} + \left[\frac{\partial \langle Y \rangle}{\partial x_i} + a\alpha_G \frac{\partial P_c^{(0)}}{\partial x_i} + aP_c^{(0)} \frac{\partial \alpha_G}{\partial x_i} \right] \frac{\partial P_{o,jk}^{(2)}}{\partial x_i} \\
&= -J_{oi} \left(Z_{21} \frac{\partial P_{c,jk}^{(2)}}{\partial x_i} + P_{c,jk}^{(2)} dZ_{21} \right) - J_{oi} \left(Z_{22} P_{c,j}^{(1)} \frac{\partial P_{c,k}^{(1)}}{\partial x_i} + Z_{22} P_{c,k}^{(1)} \frac{\partial P_{c,j}^{(1)}}{\partial x_i} + P_{c,j}^{(1)} P_{c,k}^{(1)} dZ_{22} \right. \\
&+ \frac{1}{2} Z_{23} P_{c,j}^{(1)} \frac{\partial \phi_k}{\partial x_i} + \frac{1}{2} Z_{23} P_{c,k}^{(1)} \frac{\partial \phi_j}{\partial x_i} + \frac{1}{2} Z_{23} \phi_j \frac{\partial P_{c,k}^{(1)}}{\partial x_i} + \frac{1}{2} Z_{23} \phi_k \frac{\partial P_{c,j}^{(1)}}{\partial x_i} \\
&+ \frac{1}{2} \phi_j P_{c,k}^{(1)} dZ_{23} + \frac{1}{2} \phi_k P_{c,j}^{(1)} dZ_{23} + Z_{24} \phi_j \frac{\partial \phi_k}{\partial x_i} + Z_{24} \phi_k \frac{\partial \phi_j}{\partial x_i} + \phi_j \phi_k dZ_{24} \Big) \\
&- \frac{1}{2} \frac{\partial P_{o,j}^{(1)}}{\partial x_i} \left[\frac{\partial f_k}{\partial x_i} + a\alpha_G \left(\frac{\partial P_{c,k}^{(1)}}{\partial x_i} + \phi_k \frac{\partial P_c^{(0)}}{\partial x_i} + P_c^{(0)} \frac{\partial \phi_k}{\partial x_i} \right) \right. \\
&+ a \left(P_{c,k}^{(1)} + \phi_k P_c^{(0)} \right) \frac{\partial \alpha_G}{\partial x_i} + \alpha_G \left(P_{c,k}^{(1)} + \phi_k P_c^{(0)} \right) \frac{\partial a}{\partial x_i} \Big] \\
&- \frac{1}{2} \frac{\partial P_{o,k}^{(1)}}{\partial x_i} \left[\frac{\partial f_j}{\partial x_i} + a\alpha_G \left(\frac{\partial P_{c,j}^{(1)}}{\partial x_i} + \phi_j \frac{\partial P_c^{(0)}}{\partial x_i} + P_c^{(0)} \frac{\partial \phi_j}{\partial x_i} \right) \right. \\
&+ a \left(P_{c,j}^{(1)} + \phi_j P_c^{(0)} \right) \frac{\partial \alpha_G}{\partial x_i} + \alpha_G \left(P_{c,j}^{(1)} + \phi_j P_c^{(0)} \right) \frac{\partial a}{\partial x_i} \Big], \tag{B-3}
\end{aligned}$$

with boundaries

$$\begin{aligned}
P_{o,jk}^{(2)}(\mathbf{x}) &= 0, & \mathbf{x} \in \Gamma_D, \\
n_i(\mathbf{x}) \left[\frac{\partial P_{o,jk}^{(2)}(\mathbf{x})}{\partial x_i} + \frac{1}{2} \left(Z_{o,j}^{(1)}(\mathbf{x}) \frac{\partial P_{o,k}^{(1)}(\mathbf{x})}{\partial x_i} + Z_{o,k}^{(1)}(\mathbf{x}) \frac{\partial P_{o,j}^{(1)}(\mathbf{x})}{\partial x_i} \right) \right. \\
&\quad \left. + J_{oi}(\mathbf{x}) \left(Z_{o,jk}^{(2)}(\mathbf{x}) + \frac{1}{2} Z_{o,j}^{(1)}(\mathbf{x}) Z_{o,k}^{(1)}(\mathbf{x}) \right) \right] = 0, & \mathbf{x} \in \Gamma_N,
\end{aligned}$$

where the decomposed second order phase mobility is

$$\begin{aligned}
Z_{w,jk}^{(2)}(\mathbf{x}) &= -\alpha_G \left(P_{c,jk}^{(2)} + \frac{1}{2} \phi_j P_{c,k}^{(1)} + \frac{1}{2} \phi_k P_{c,j}^{(1)} + \frac{1}{2} \phi_j \phi_k P_c^{(0)} \right), \\
Z_{o,jk}^{(2)}(\mathbf{x}) &= Z_{21} P_{c,jk}^{(2)} + Z_{22} P_{c,j}^{(1)} P_{c,k}^{(1)} + \frac{1}{2} Z_{23} \left(\phi_j P_{c,k}^{(1)} + \phi_k P_{c,j}^{(1)} \right) + Z_{24} \phi_j \phi_k.
\end{aligned}$$

Note that the above second order terms are written in a symmetric style.

References

- Abdin, E and Kaluarachchi, J (1997a). Stochastic analysis of three-phase flow in heterogeneous porous media: 1. Spectral/perturbation approach. *Water Resources Research* 33(7): 1549-1558.
- Abdin, E and Kaluarachchi, J (1997b). Stochastic analysis of three-phase flow in heterogeneous porous media: 2. Numerical simulations. *Water Resources Research* 33(7): 1559-1566.
- Abriola, L (1989). Modeling multiphase migration of organic chemicals in groundwater systems - A review and assessment. *Environmental Health Perspectives* 83: 117-143.
- Bakr, A , Gelhar, W, Gutjahr, L, and MacMillan, R (1978). Stochastic analysis of spatial variability in subsurface flow. 1: Comparison of one- and three-dimensional flows. *Water Resources Research* 14:263-271.
- Bear, J. (1972). *Dynamics of Fluids in Porous Media*, Dover., New York.
- Chang, C (1995). Stochastic Analysis of Two-Phase Flow in Porous Media: I. Spectral/Perturbation Approach. *Transport in Porous Media* 19: 233-259.
- Cheng, A and Lape, D (1991). Boundary element solution for stochastic groundwater flow: Random boundary condition and recharge. *Water Resources Research* 27(2):231-242.
- Courant and Hilbert (1953). *Methods of Mathematical Physics*. Interscience, New York.
- Dagan, G (1989). *Flow and Transport in Porous Formations*, Springer-Verlag. New York.
- Deutsch, C and Journel, A (1998). *GSLIB, Geostatistical Software Library and User's Guide*, Second Edition. Oxford University Press. New York.
- Garg, S and Rixey, G (1999). The dissolution of benzene, toluene, m-xylene and naphthalene from a residually trapped non-aqueous phase liquid under mass transfer limited conditions. *Journal of Contaminant Hydrology* 36(3-4): 313-331.
- Gelhar, W (1993). *Stochastic Subsurface Hydrology*, Prentice-Hall, Englewood Cliffs, NJ.
- Ghanem, R and Spanos, D. (1991) *Stochastic Finite Elements: a Spectral Approach*. New York, Springer-Verlag.
- Ghanem, R and Dham, S (1998). Stochastic Finite Element Analysis for Multiphase Flow in Heterogeneous Porous Media. *Transport in Porous Media* 32:239-262.

- Guadagnini, A, and Neuman, P (1999). Nonlocal and localized analyses of conditional mean steady state flow in bounded, randomly nonuniform domains: 1. Theory and computational approach. *Water Resources Research* 35(10): 2999-3018.
- Gutjahr, L, and Gelhar, W (1981). Stochastic models of subsurface flow: infinite versus finite domains and stationarity. *Water Resources Research* 17: 337-350.
- Karhunen, K (1947). Über lineare methoden in der wahrschein-lichkeitsrechnung. *Amer. Acad. Sci.*, Fennicade, Ser. A, I, Vol 37: 3-79. (Translation: RAND Corporation, Santa Monica, California, Rep. T-131, Aug. 1960).
- Loeve, M (1948). *Fonctions aleatoires du second ordre, supplement to P. Levy*. Processus Stochastic et Mouvement Brownien, Paris, Gauthier, Villars.
- Loeve, M (1977). *Probability Theory*, 4th edition. Springer-Verlag, Berlin.
- Lu, Z and Zhang, D (2004). A comparative study on uncertainty quantification for flow in random heterogeneous media using Monte-Carlo simulations, the conventional and KL-based moment equations approach. *SIAM, Journal of Scientific Computing*, in press.
- Keller, A, Blunt, M and Roberts, P (2000). Behavior of Dense Non-Aqueous Phase Liquids in fractured porous media under two-phase flow conditions. *Transport in Porous Media* 38: 189-203.
- Keller, A and Chen, M (2002). *Seasonal variation in bioavailability of residual NAPL in the vadose zone*. International Groundwater Symposium, Berkeley, CA, USA, IAHS.
- Kram, M, Keller, A, Rossabi, J and Everett, L (2001). DNAPL Characterization Methods and Approaches Part 1: Performance Comparisons. *Ground Water Monitoring and Remediation*, 21(1): 67-76.
- Mercer, W and Cohen, M (1990). A review of immiscible fluids in the subsurface: properties, models, characterization and remediation. *J. of Contaminant Hydrology* 6: 107-163.
- Neuman, P, and Orr, S (1993). Prediction of steady state flow in non-uniform geologic media by conditional moments: Exact non-local formalism, effective conductivities, and weak approximation. *Water Resources Research* 29(2): 341-364.
- Osnes, H (1995). Stochastic analysis of head spatial variability in bounded rectangular heterogeneous aquifers. *Water Resources Research* 31(12): 2981-2990.

- Rubin, Y and Dagan, G (1988). Stochastic analysis of boundaries effects on head spatial variability in heterogeneous aquifers: 1.Constant head boundary. *Water Resources Research* 24(10): 1689-1697.
- Rubin, Y and Dagan, G (1989). Stochastic analysis of boundaries effects on head spatial variability in heterogeneous aquifers: 2.Impervious boundary. *Water Resources Research* 25(4): 707-712.
- Tartakovsky, M, and Neuman, P (1998). Transient flow in bounded randomly heterogeneous domains: 1. Exact conditional moment equations and recursive approximations. *Water Resources Research* 34(1): 13-20.
- van Genuchten (1980). A closed-form equation for predicting the hydraulic conductivity of unsaturated soils. *Soil Sci. Soc. Am. J.* 44: 892-898.
- Weiner, N (1930). The homogeneous chaos. *Amer. J. Math* 60:897-936.
- Yang, J, Zhang, D, and Lu, Z (2004). Stochastic analysis of saturated-unsaturated flow in heterogeneous media by combing Karhunen-Loeve expansion and perturbation method. *Journal of Hydrology*, in press.
- Zhang, D (1998). Numerical solutions to statistical moment equations of groundwater flow in non-stationary, bounded, heterogeneous media. *Water Resources Research* 34(3): 529-538.
- Zhang, D, and Winter, L (1998). Moment-Equation approach to single-phase fluid flow in heterogeneous reservoirs. *SPE Journal* 4(2): 118-127.
- Zhang, D (1999). Non-stationary stochastic analysis of transient unsaturated flow in randomly heterogeneous media. *Water Resources Research* 35(4): 1127-1141.
- Zhang, D (2002). *Stochastic Methods for Flow in Porous Media: Coping with Uncertainties*, Academic Press, San Diego, Calif., ISBN 012-7796215, pp.350.
- Zhang, D and Lu, Z (2002). Stochastic analysis of flow in a heterogeneous unsaturated-saturated system. *Water Resources Research* 38(2): 101-1015.
- Zhang, D, and Lu Z (2004). Evaluation of Higher-Order Moments for Saturated Flow in Randomly Heterogeneous Media via Karhunen-Loeve Decomposition. *Journal of Computational Physics* 194(2): 773-794.
- Zhang, D and Sun, A (2000). Stochastic analysis of transient saturated flow through heterogeneous fractured porous media: A double-permeability approach. *Water Resources Research* 36(4): 865-874.

Table 1 Soil and fluid properties and boundary conditions

Parameter name	Symbol	Units	Case 1	Case 2
Water density	ρ_w	kg/m ³	1000	1000
Oil density	ρ_o	kg/m ³	400	400
Water viscosity	μ_w	Pa·s	1.0x10 ⁻³	1.0 x10 ⁻³
Oil viscosity	μ_o	Pa·s	6.5x10 ⁻⁴	6.5 x10 ⁻⁴
Mean log permeability	$\langle Y \rangle$	ln(m ²)	-33.0	-33.0
Mean log pore size distribution	$\langle \beta \rangle$	ln(1/Pa)	-9.0	-9.0
Variance log permeability	σ_Y^2	-	0.25	0.81
Variance log pore size distribution	σ_β^2	-	0.01	0.01
Coefficient of variation (k)	$CV(k)$	-	53%	112%
Coefficient of variation (α)	$CV(\alpha)$	-	10%	10%
Correlation length	η_Y, η_β	m	0.3	0.3
Upper boundary water flux	Q_w	m/s	6.8x10 ⁻⁹	1.0x10 ⁻¹⁰
Upper boundary oil flux	Q_o	m/s	2.4x10 ⁻⁸	1.0x10 ⁻¹⁰
Low boundary water pressure	P_w	Pa	1.0x10 ⁵	1.0x10 ⁵
Low boundary oil pressure	P_o	Pa	1.16x10 ⁵	1.5x10 ⁵

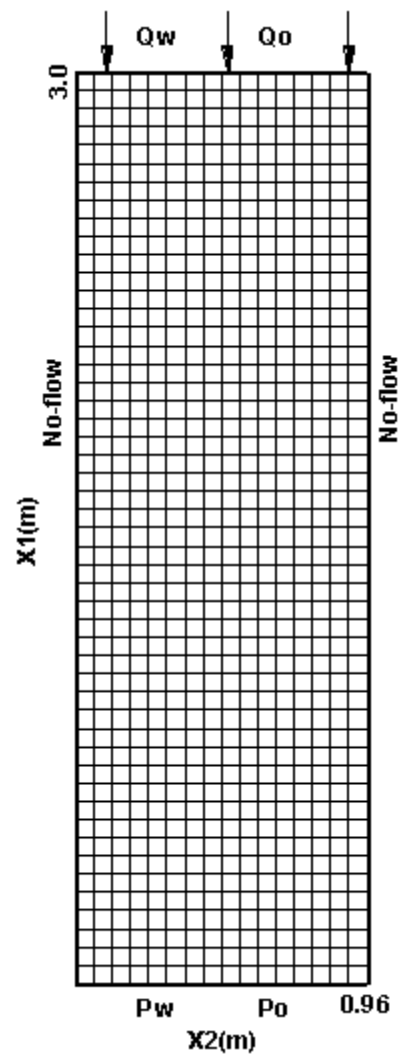


Fig.1 Domain and Boundary

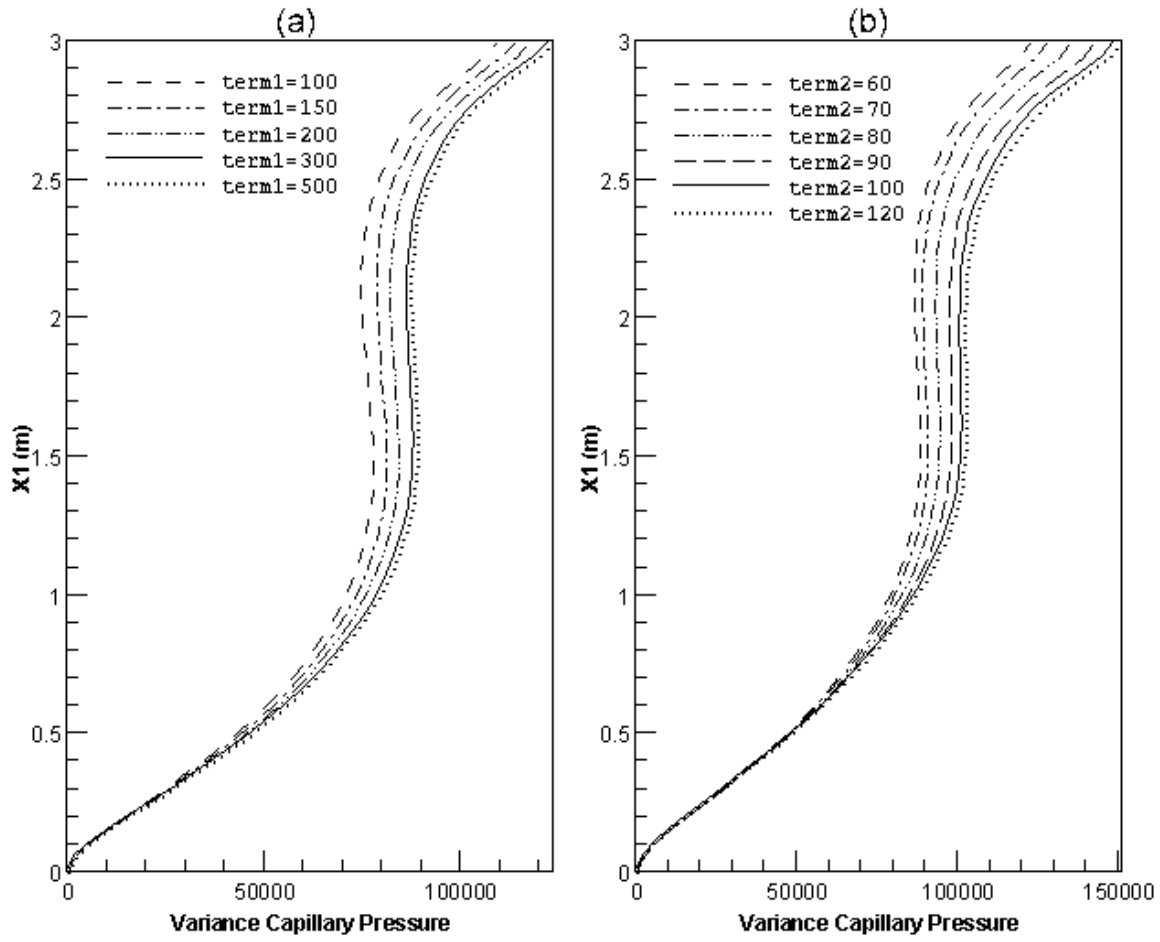


Fig. 2. P_c variance along central vertical cross-section: (a) fixed $term2=60$, different $term1$; (b) fixed $term1=300$, different $term2$.

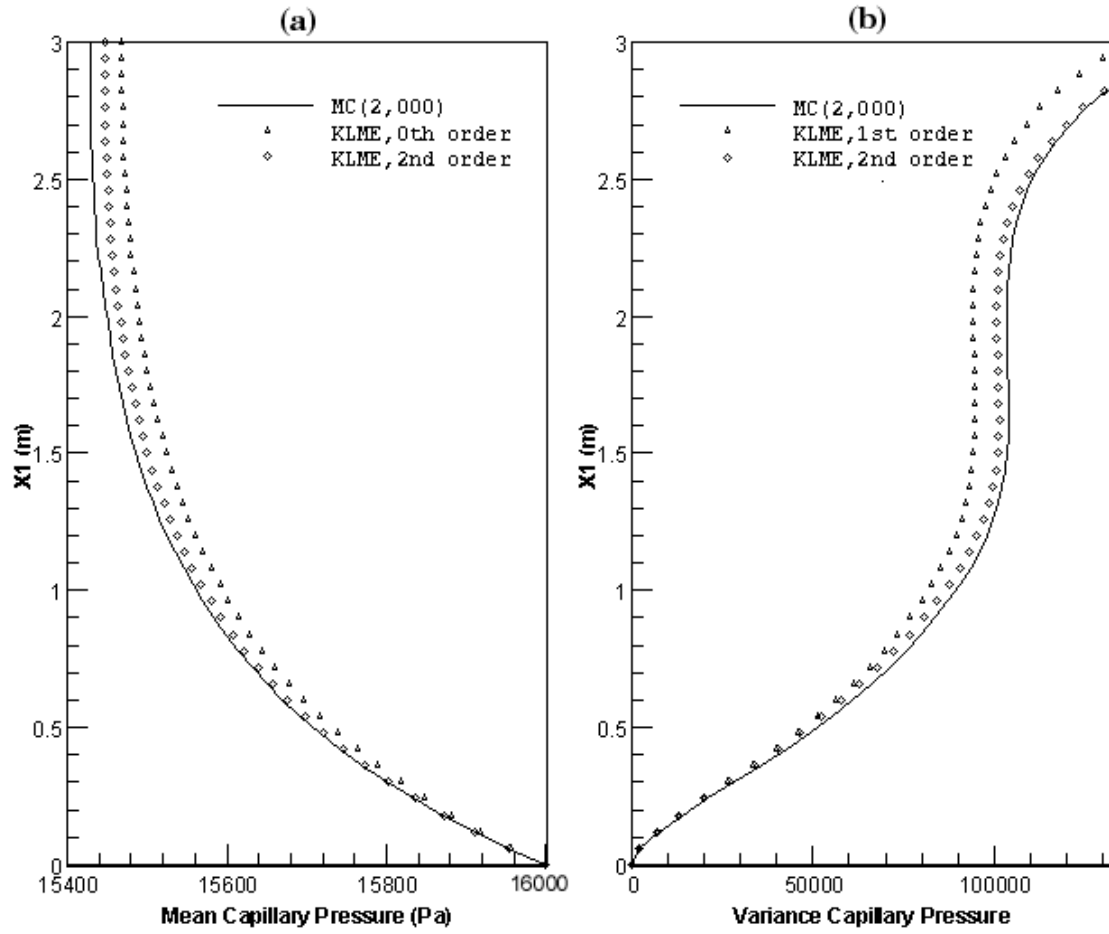


Fig. 3. Comparison of capillary pressure (P_c) in Case 1 (along central vertical cross-section) between KLME and Monte Carlo simulation: (a) mean P_c ; (b) variance of P_c .

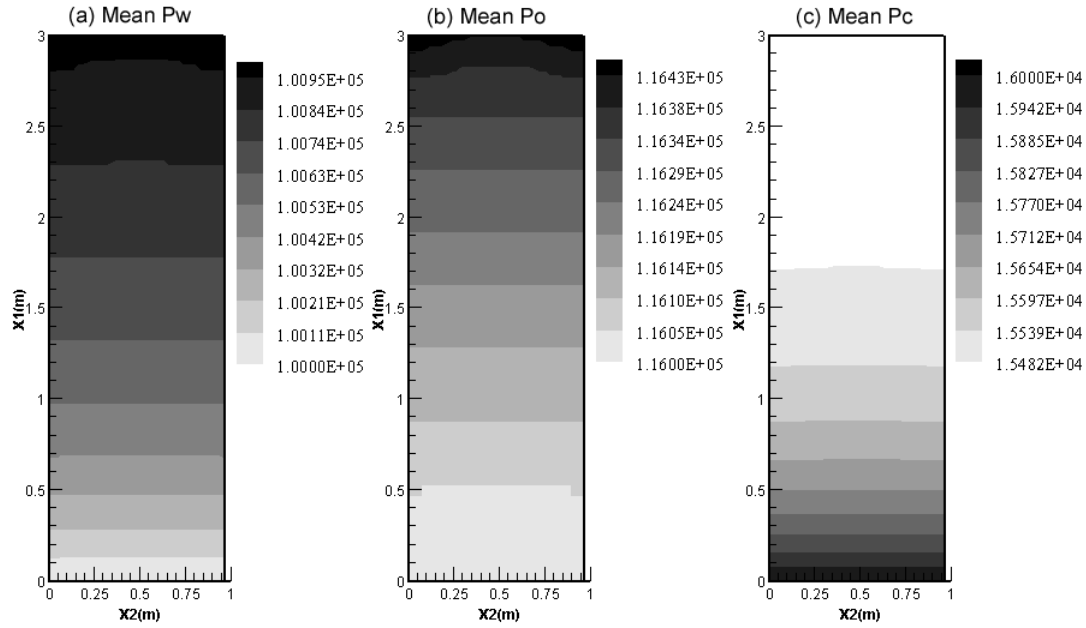


Fig. 4. Contour map of mean fluid pressure and capillary pressure (Pa) in Case 1: (a) water phase; (b) oil phase; (c) capillary pressure.

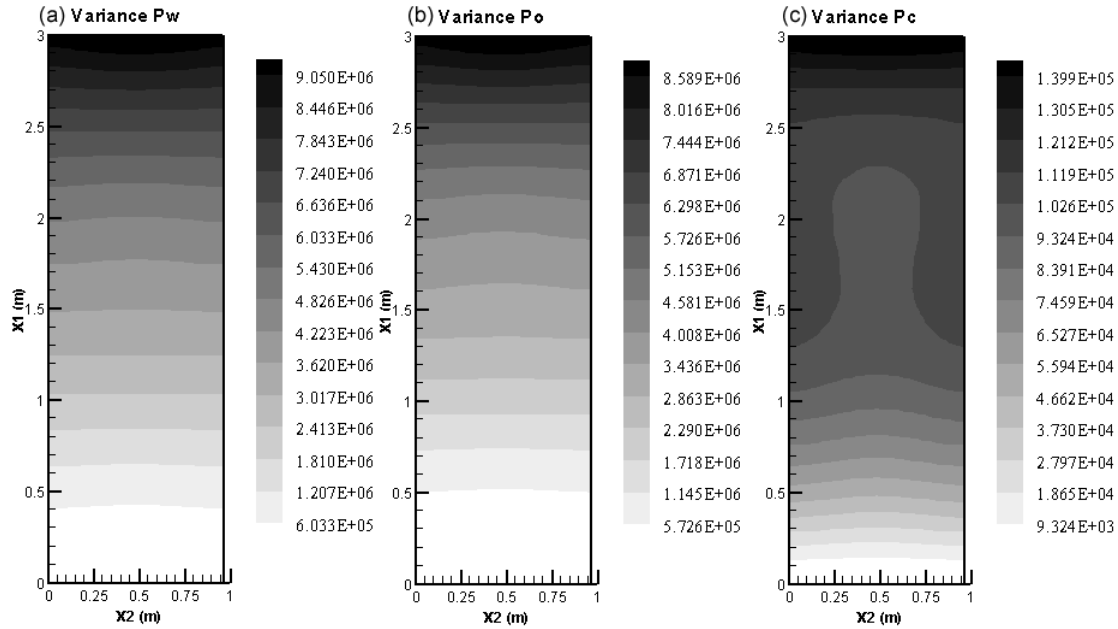


Fig. 5. Contour map of variance of fluid pressure and capillary pressure in Case 1: (a) water phase; (b) oil phase; (c) capillary pressure.

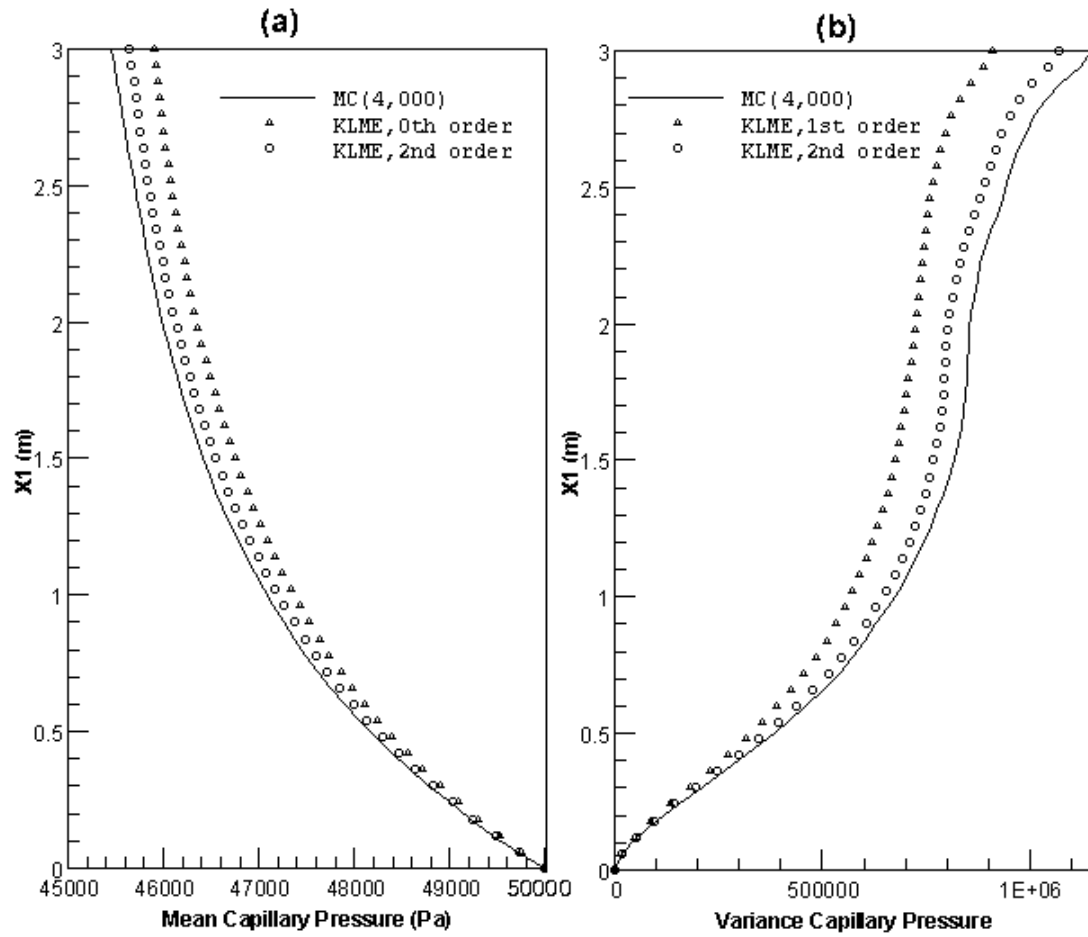


Fig. 6. Comparison of capillary pressure (Pc) in Case 2 (along central vertical cross-section) between KLME and Monte Carlo (MC) simulation: (a) mean Pc; (b) variance Pc.

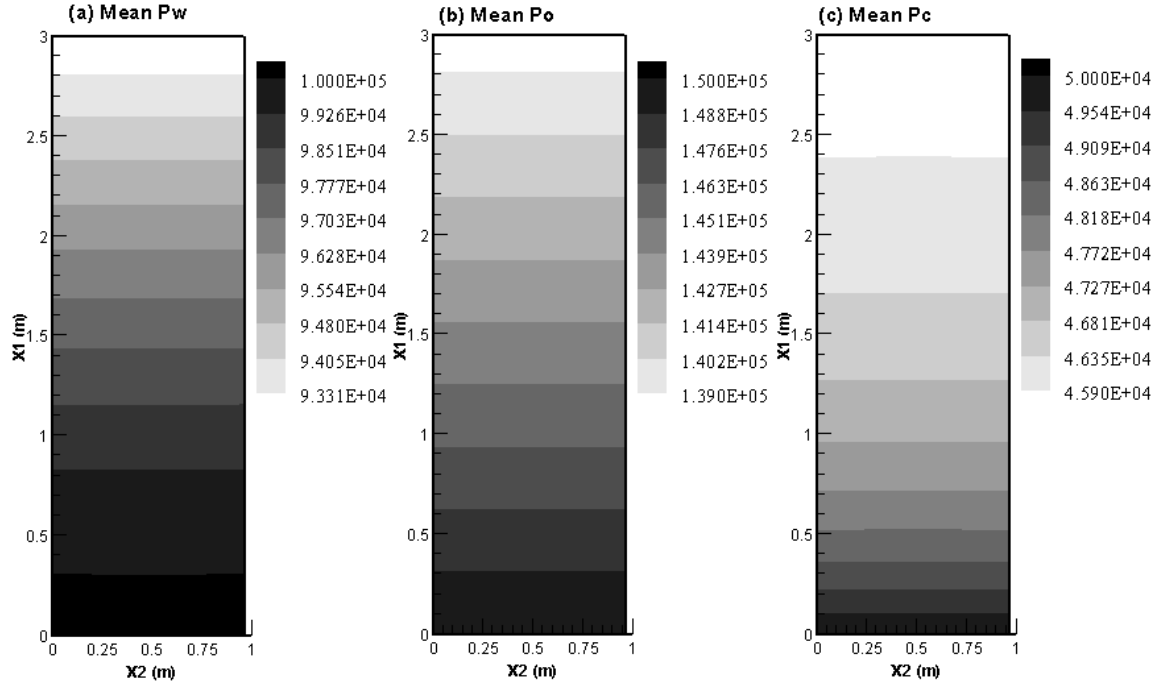


Fig. 7. Contour map of mean fluid pressure and capillary pressure (Pa) in Case 2:
(a) water phase; (b) oil phase; (c) capillary pressure.

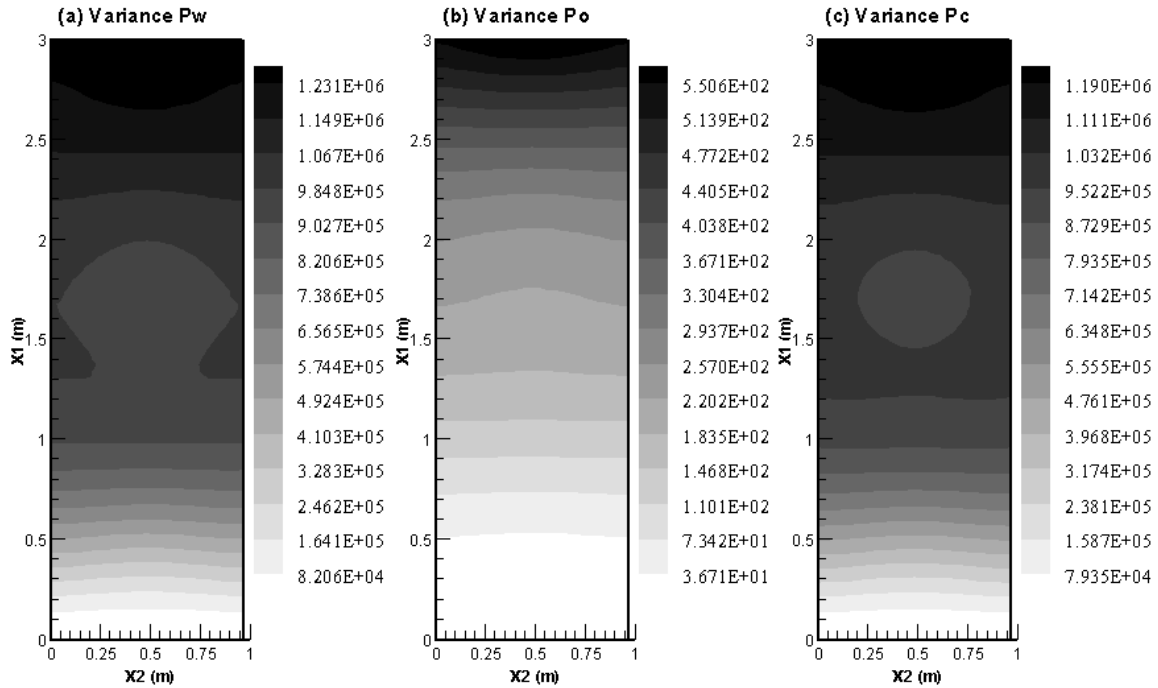


Fig. 8. Contour map of variance of fluid pressure and capillary pressure in Case 2:
(a) water phase; (b) oil phase; (c) capillary pressure.